

Highly π -Extended TTF Analogues with a Conjugated Macrocyclic Enyne Core

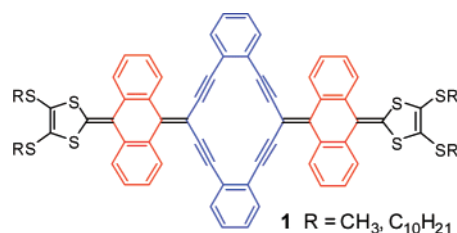
Guang Chen, Li Wang, David W. Thompson, and Yuming Zhao*

Department of Chemistry, Memorial University of Newfoundland, St. John's, Newfoundland A1B 3X7, Canada

yuming@mun.ca

Received December 18, 2007

ABSTRACT



The synthesis of a class of highly π -extended tetrathiafulvalene derivatives (1a and 1b) was explored using Sonogashira macrocyclization as a key step. The solid-state structure of 1b was characterized by X-ray single crystallography, showing a substantially bent, S-shaped molecular backbone and an ordered packing geometry in a π -alkyl–alkyl- π stacking fashion. Electronic and redox properties of 1b were investigated by UV–vis absorption, fluorescence spectroscopy, and cyclic voltammetry.

Synthesis of π -extended tetrathiafulvalene analogues (exTTFs) has been an intense and active area in the research of organic electronic materials.¹ For the design of various TTF derivatives, insertion of π -conjugated spacers such as vinylogous and/or acene units in between the two dithiole rings of a TTF parent structure constitutes a popular and effective approach.^{1a,2} A prominent class of exTTFs derived from this approach is the quinonoid-type exTTFs,^{1,2a–g} which usually exhibit significantly enhanced electron-donating and charge-transfer properties as well as extensive applications in molecular optoelectronic materials and devices.

Lately, much attention has been devoted to the use of structurally complex and highly extended π -conjugated

systems as central π -spacers for new exTTF variants. Martín and co-workers in 2005 reported a class of exTTFs containing a unique spiroconjugated central core.³ In 1991, Bryce's group synthesized a series of bianthro-TTFs,⁴ which were later thoroughly investigated by Guldi and co-workers.⁵ Nielsen⁶ and Diederich⁷ have developed a class of conjugated enyne oligomer bridged exTTFs, while most recently a sophisticated cyclic aromatic structure, truxene, was employed by the Martín group to generate a type of truxene-cored exTTFs.⁸

Among the numerous π -conjugated cyclic and acyclic structural motifs that have been employed as spacers for

(1) (a) Bendikov, M.; Wudl, F.; Perepichka, D. F. *Chem. Rev.* **2004**, *104*, 4891. (b) Segura, J. L.; Martín, N. *Angew. Chem., Int. Ed.* **2001**, *40*, 1371 and references cited therein. (c) Bryce, M. R.; Moore, A. J. *Pure Appl. Chem.* **1990**, *62*, 473–476.

(2) For selected recent examples, see: (a) Christensen, C. A.; Batsanov, A. S.; Bryce, M. R. *J. Org. Chem.* **2007**, *72*, 1301. (b) Christensen, C. A.; Batsanov, A. S.; Bryce, M. R. *J. Am. Chem. Soc.* **2006**, *128*, 10484. (c) Díaz, M. C.; Illescas, B. M.; Martín, N.; Perepichka, I. F.; Bryce, M. R.; Levillain, E.; Viruela, R.; Ortí, E. *Chem.-Eur. J.* **2006**, *12*, 2709. (d) Hudhomme, P.; Sallé, M.; Gautier, N.; Belyasmine, A.; Gorgues, A. *Arkivoc* **2006**, 49. (e) Christensen, C. A.; Bryce, M. R.; Batsanov, A. S.; Becher, J. *Org. Biomol. Chem.* **2003**, *1*, 511. (f) Díaz, M. C.; Illescas, B. M.; Seoane, C.; Martín, N. *J. Org. Chem.* **2004**, *69*, 4492. (g) Díaz, M. C.; Illescas, B.; Martín, N. *Tetrahedron Lett.* **2003**, *44*, 945. (h) Frère, P.; Boubekeur, K.; Jubault, M.; Batail, P.; Gorgues, A. *Eur. J. Org. Chem.* **2001**, 3741.

(3) Sandín, P.; Martínez-Grau, A.; Sánchez, L.; Seoane, C.; Pou-Américo, R.; Ortí, E.; Martín, N. *Org. Lett.* **2005**, *7*, 295–298.

(4) Moore, A. J.; Bryce, M. R. *J. Chem. Soc., Perkin Trans. 1* **1991**, 157.

(5) Díaz, M. C.; Illescas, B. M.; Martín, N.; Viruela, R.; Viruela, P. M.; Ortí, E.; Brede, O.; Zilbermann, I.; Guldi, D. M. *Chem.—Eur. J.* **2004**, *10*, 2067.

(6) (a) Ryhding, T.; Petersen, M. Å.; Kilså, K.; Nielsen, M. B. *Synlett* **2007**, 913. (b) Sørensen, J. K.; Vestergaard, M.; Kadziola, A.; Kilså, K.; Nielsen, M. B. *Org. Lett.* **2006**, *8*, 1173. (c) Anderson, A. S.; Qvortrup, K.; Torbensen, E. R.; Mayer, J.-P.; Gisselbrecht, J.-P.; Boudon, C.; Gross, M.; Kadziola, A.; Kilså, K.; Nielsen, M. B. *Eur. J. Org. Chem.* **2005**, 3660. (d) Qvortrup, K.; Jakobsen, M. T.; Gisselbrecht, J.-P.; Boudon, C.; Jensen, F.; Nielsen, S. B.; Nielsen, M. B. *J. Mater. Chem.* **2004**, *14*, 1768.

(7) Nielsen, M. B.; Utesch, N. F.; Moonen, N. N. P.; Boudon, C.; Gisselbrecht, J.-P.; Concilio, S.; Piotto, S. P.; Seiler, P.; Günter, P.; Gross, M.; Diederich, F. *Chem. Eur. J.* **2002**, *8*, 3601.

exTTFs, conjugated enyne macrocycles are still relatively unexplored, despite the fact that conjugated macrocycles have been known to possess many attractive properties of both theoretical and practical value to supramolecular, biological, and materials science.⁹ To shed more light on this issue, a new type of highly π -extended TTF analogues **1** (Figure 1)

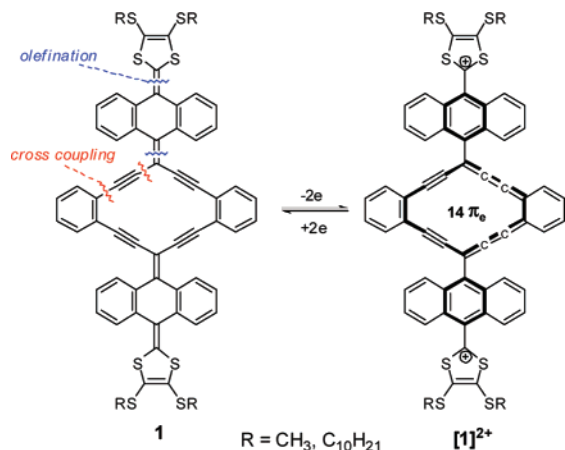


Figure 1. Molecular structures of compounds **1** in neutral and dicationic states.

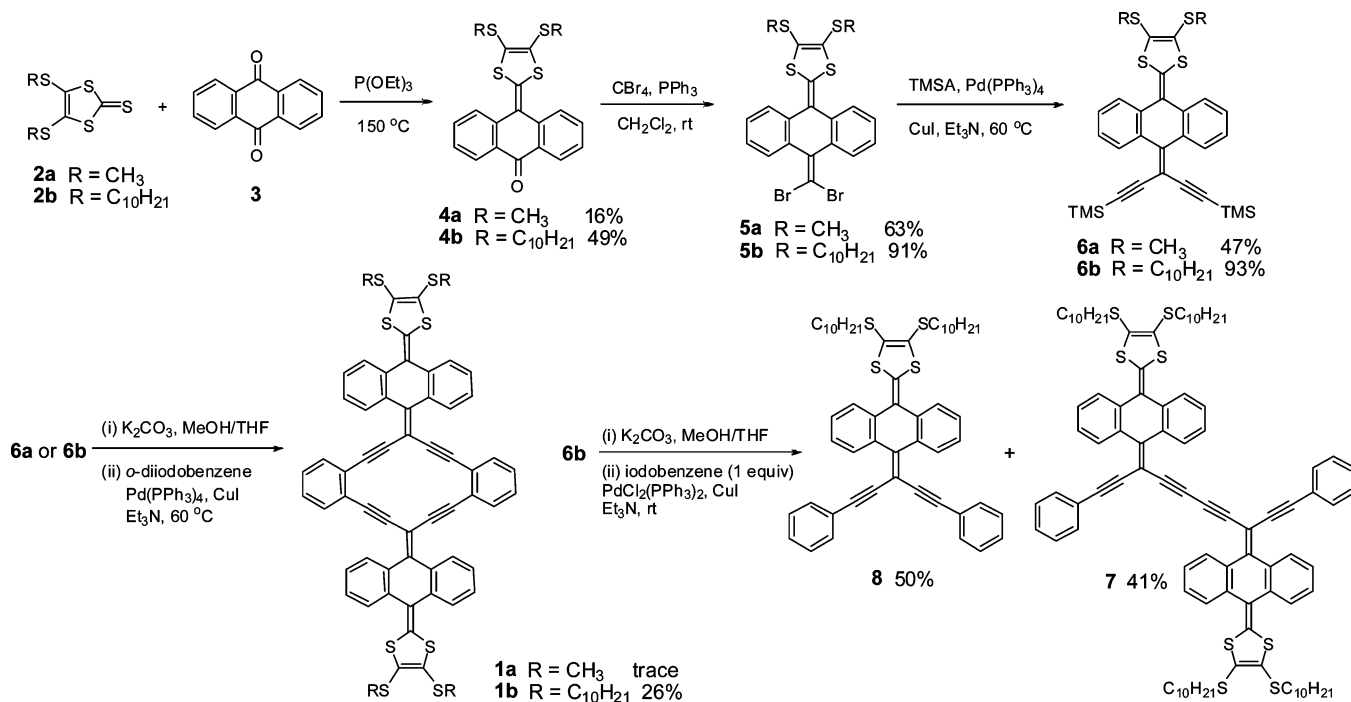
are introduced below, whose main structural features include a conjugated bisbenzo enyne macrocycle core and two dianthro units.

Incorporation of the enyne macrocyclic unit would represent a significant step in the development of novel TTF-

containing organic materials. Fundamentally important knowledge on the π -electron delocalization pattern and aromatic characteristics associated with the conjugated enyne cyclic systems¹⁰ in both neutral and oxidized (e.g., dicationic) states can be rigorously established by both theoretical and experimental methods. On the other hand, the unique optoelectronic properties arising from the enyne macrocycle unit^{9a,b,e} and possible reactivity of Bergman-type cyclization at the endiynes fragments¹¹ may create new avenues for other synthetic ventures and practical explorations.

Construction of such a complex conjugated system as **1** is not trivial and requires prudent choice of efficient synthetic routes to prepare dithiolenyl-acene precursors and suitable ring closure strategies to build the enyne macrocycle. In this work, a convergent route using iterative olefination and metal-catalyzed cross-coupling reactions as key steps was employed. A brief retrosynthetic bond disconnection analysis is given in Figure 1, while detailed synthetic steps are outlined in Scheme 1. The synthesis began with a reaction between thione **2a** or **2b**¹² with excess anthraquinone **3** in triethyl phosphite at 150 °C, yielding ketones **4a** and **4b**, respectively. This methodology originally developed by Bryce^{2a} turned out to be particularly effective in the synthesis of long-alkyl chain substituted compound **4b**. Compounds **4a,b** were then subjected to a Corey–Fuchs reaction to afford dibromides **5a** and **5b**. A Sonogashira coupling between **5** and trimethylsilylacetylene (TMSA) under Pd/Cu catalysis resulted in compounds **6a,b**. Finally, compounds **6a** and **6b** were reacted with *o*-diiodobenzene via a Sonogashira-type high-dilution macrocyclization protocol, furnishing the desired products **1a** and **1b**. Besides the cyclization product, various acyclic oligomeric byproducts were also formed in

Scheme 1. Synthesis of exTTFs **1** and Reference Compound **8**



this reaction as characterized by MALDI-TOF MS analysis. The yield of **1a** was trace, and complete isolation of **1a** from concomitant byproducts by flash column chromatography was not tenable. The low yield and difficulty encountered in purification of **1a** could be a consequence of the poor solubility of the methyl-substituted exTTF **1a**. For *n*-decyl chain decorated exTTF **1b**, the solubility was dramatically increased, and a better yield of 26% was achieved in the macrocyclization step. Compound **1b** was thoroughly purified by silica flash column chromatography and then fully characterized by IR, ¹H and ¹³C NMR, and MS analyses. In addition to exTTFs **1a,b**, a reference compound **8** was also prepared for comparison purposes via cross-coupling desilylated **6b** with excess iodobenzene under Pd/Cu catalysis. Interestingly, when a 1:1 molar ratio of desilylated **6b** and iodobenzene was applied in this coupling reaction, a significant amount of homo-cross-coupled byproduct **7** was also produced, which can be viewed as well as an exTTF variant extended by acene and acyclic cross-conjugated oligo(enyne) π -spacers.^{6,7}

Single crystals of **1b** were grown through slow diffusion of MeOH into a CHCl₃ solution of **1b** at 4 °C. The crystal structure of **1b** was then investigated by X-ray crystallographic analysis. Two structurally similar polymorphs were observed in the single crystal of **1b**. Figure 2a shows the

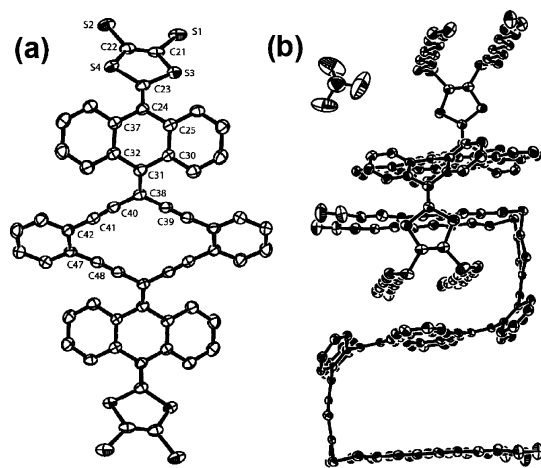


Figure 2. (a) ORTEP drawing of compound **1b** at the 50% probability level (*n*-decyl chains were removed for clarity). (b) Solid-state packing of two molecules of **1b** in the unit cell. Selected bond lengths (Å): C23–C24 1.361(5), C24–C37 1.474(6), C32–C37 1.410(5), C31–C32 1.478(7), C31–C38 1.374(7), C38–C40 1.431(5), C40–C41 1.189(5), C41–C42 1.439(5), C42–C47 1.429(7). Selected bond angles (deg): C25–C24–C37 114.9(3), C30–C31–C32 113.8(4), C39–C38–C40 113.9(4), C38–C40–C41 174.3(6), C40–C41–C42 175.2(5), C41–C42–C47 121.1(4).

ORTEP plot highlighting the geometric features of the conjugated molecular skeletons for one of the polymorphs. Compound **1b** displays a substantially bent “S”-shaped structure, in which the central macrocyclic enyne assumes a

planar conformation, while the two dithiole rings are in a nearly perpendicular orientation versus the central cyclic enyne plane. The interplanar angle between the two planes of adjacent dithiole and anthracene units is measured at 15.5°, while the angle between the dithiole ring and central cyclic enyne plane is at 79.3°. These angles are in line with those bend parameters observed in the crystal structures of quinoindimethane-type exTTFs.^{2a,e}

In the crystal lattice, two molecules of **1b** are closely positioned in a manner as depicted in Figure 2b. The chain length of *n*-decyl groups in **1b** and the central bisbenzocyclic enyne moiety effect a π -alkyl-alkyl- π intermolecular stacking,^{2c} interlocking the two molecules orthogonally with respect to one another.

Electronic properties of **1b** and its “half-structure”, compound **8**, were investigated by UV–vis and fluorescence spectroscopic methods. Comparison of the properties of **1b** and **8** has disclosed essential information with respect to structure–property relationship. Figure 3a shows the UV–

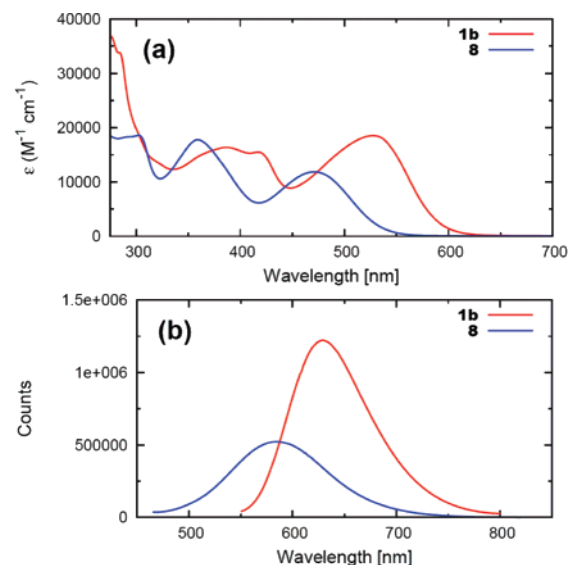


Figure 3. (a) UV–vis absorption spectra of **1b** and **8** measured in CHCl₃. (b) Fluorescence spectra of **1b** ($\lambda_{\text{ex}} = 531$ nm, $\Phi = 0.13$) and **8** ($\lambda_{\text{ex}} = 447$ nm, $\Phi = 0.064$) measured in degassed CHCl₃.

vis spectra of **1b** and **8**. Compound **1b** exhibits three significant absorption bands at 528, 419, and 387 nm, respectively, while reference **8** shows only two absorption

(9) (a) Gholami, M.; Tykwinski, R. R. *Chem. Rev.* **2006**, *106*, 4997. (b) Kar, M.; Basak, A. *Chem. Rev.* **2007**, *107*, 2861. (c) Nielsen, M. B.; Diederich, F. *Chem. Rev.* **2005**, *105*, 1837. (d) Iyoda, M.; Kuwatani, Y.; Yamagata, S.; Nakamura, N.; Todaka, M.; Yamamoto, G. *Org. Lett.* **2004**, *6*, 4667. (e) Zhao, T.; Liu, Z.; Song, Y.; Xu, W.; Zhang, D.; Zhu, D. *J. Org. Chem.* **2006**, *71*, 7422.

(10) (a) Lepetit, C.; Godard, C.; Chauvin, R. *New J. Chem.* **2001**, *25*, 572–580. (b) Maurette, L.; Godard, C.; Frau, S.; Lepetit, C.; Soleilhavoup, M.; Chauvin, R. *Chem.–Eur. J.* **2001**, *7*, 1165. (c) Matzger, A. J.; Vollhardt, K. P. C. *Tetrahedron Lett.* **1998**, *39*, 6791. (d) Chauvin, R. *Tetrahedron Lett.* **1995**, *36*, 397–400.

(11) (a) Treitel, N.; Eshdat, L.; Sheradsky, T.; Donovan, P. M.; Tykwinski, R. R.; Scott, L. T.; Hopf, H.; Rabinovitz, M. *J. Am. Chem. Soc.* **2006**, *128*, 4703. (b) Rawat, S.; Zaleski, J. M. *Synlett* **2004**, 393.

(8) Pérez, E. M.; Sierra, M.; Sánchez, L.; Torres, M. R.; Viruela, R.; Viruela, P. M.; Ortíz, E.; Martín, N. *Angew. Chem., Int. Ed.* **2007**, *46*, 1847.

bands at 446 and 347 nm. The lowest-energy absorption band of **1b**, relative to that of its half-structure **8**, has substantially red-shifted by ca. 3482 cm^{-1} , indicating that the HOMO–LUMO gap of **1b** has been substantially reduced due to the extensive π -delocalization at the central enyne cyclic conjugated unit.

The fluorescent properties of **1b** and **8** are delineated in Figure 3b. The maximum emission peak (λ_{em}) of **1b** appears at 628 nm, a wavelength red-shifted by 44 nm (1200 cm^{-1}) versus that of **8** (584 nm). This observation is consistent with the UV–vis results which show that exTTF **1b** has smaller HOMO–LUMO gap than does **8**. The fluorescence quantum yield of **1b** ($\Phi = 0.13$) is about double that of its half-structure **8** ($\Phi = 0.064$), which is counterintuitive with respect to expectations based on energy gap laws. Detailed Franck–Condon line-shape analyses as a function of temperature¹³ are currently underway to characterize the lowest lying emitting state.

Electrochemical redox properties of **1b** and **8** were characterized by cyclic voltammetry (see Figure 4 and Table

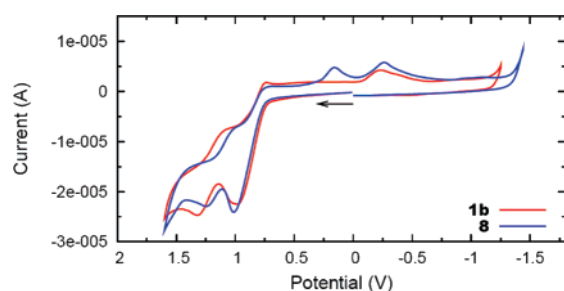


Figure 4. Cyclic voltammograms of **1b** and **8** as measured in $\text{CHCl}_3/\text{CH}_3\text{CN}$ (4:1, v/v) at room temperature. Bu_4NBF_4 (0.1 M) as the supporting electrolyte, glassy carbon as the working electrode, Pt wire as the counter electrode, and Ag/AgCl as the reference. Scan rate: 0.1 V s^{-1} .

1). Scanning cathodically, **1b** and **8** both show an irreversible cathodic peak current at similar potentials. The origin of this current peak is not clear and waits for further investigations.

- (12) (a) Moore, A. J.; Bryce, M. R. *Tetrahedron Lett.* **1992**, 33, 1373.
 (b) Chen, G.; Zhao, Y. *Tetrahedron Lett.* **2006**, 47, 5069.
 (13) Chen, P.; Meyer, T. J. *Chem. Rev.* **1998**, 98, 1439.

Table 1. Redox Potential Data of Compounds **1b** and **8** (vs Ag/AgCl)

entry	oxidation (V)		reduction (V)	
	E_{pa}	E_{pc}	E_{pa}	E_{pc}
1b	0.98, 1.32	0.73, 1.10	–0.23	
8	1.01, 1.25	0.16, 1.02	–0.26	

In the oxidation region, two irreversible redox wave pairs are discernible in both compounds. The redox potentials are very similar except for the first cathodic peak potential. For compound **8**, the value has dramatically shifted to 0.16 V relative to that of exTTF **1b** at 0.73 V. The resemblance of **1b** and **8** in oxidation profile indicates that exTTF **1b** retains an electron-donating ability quite similar to its half-structure **8**. The loss of TTF-like electron donating ability in **1b** can be presumably attributed to the substantial energy cost required to planarize its highly bent structure upon oxidation.

In summary, we have developed a new synthetic entry to a class of dianthro–enyne macrocycle based exTTF derivatives. Insertion of macrocyclic enyne π -spacer into TTF has brought about interesting solid-state packing and electronic absorption/emission properties to exTTF **1b**, but rendered it a poorer electron-donor than those exTTFs with relatively shorter π -spacers.^{2–8} Nevertheless, this work represents the first experimental exploration of such type of exTTFs, and will serve useful guidance in further quest for new molecular hybrids made up of TTF and conjugated cyclic oligo(enyne) building blocks.

Acknowledgment. We acknowledge the support from the Natural Sciences and Engineering Research Council of Canada (NSERC), Canadian Foundation for Innovation (CFI), and Memorial University of Newfoundland. Ms. Julie Collins and Ms. Louise Dawe of Memorial University are acknowledged for assistance in X-ray structural analysis, and Dr. Chris Flinn of Memorial University is acknowledged for very helpful discussions.

Supporting Information Available: Experimental procedures, synthetic and spectroscopic data for new compounds, and a CIF file for **1b**. This material is available free of charge via the Internet at <http://pubs.acs.org>.

OL703038M